Vol. 77: 65–77, 2016
doi: 10.3354/ame01788

AQUATIC MICROBIAL ECOLOGY
Aquat Microb Ecol

Published online August 12

Microscale distributions of freshwater planktonic viruses and prokaryotes are patchy and taxonomically distinct

Lisa M. Dann[1,*], Renee J. Smith[1], Shanan S. Tobe[1], James S. Paterson[1], Rod L. Oliver[2], James G. Mitchell[1]

[1]School of Biological Sciences at Flinders University, Adelaide, South Australia 5001, Australia
[2]CSIRO Land and Water Waite Research Institute, Urrbrae, South Australia 5064, Australia

ABSTRACT: Microscale microbial distributions are patchy, with abundance hotspots and coldspots that provide important microenvironments for microbial interactions. However, studies are often restricted to abundance estimates alone. At the riverbed of the Murray River, we used taxonomy to complement quantitative analysis to show that abundance hotspots, coldspots and background levels are taxonomically distinct at all taxonomic levels. Abundance hotspots varied 115- and 5.9-fold above background over 0.9 cm for viruses and bacteria, respectively. For bacteria, hotspots represent increases in particular taxa rather than in all bacteria. Genera with increased abundances — *Pseudomonas, Parasporobacterium, Lachnospiraceae* incertae sedis and *Bacteroides* — were indicative of human and animal inputs, and represented up to 14.7% of the community. Distinct dominant genera led to high taxonomic dissimilarity among hotspots. Genera exclusivity was still higher in the background and coldspots, with 54 and 48 exclusive genera compared to 7 and 4 genera in hotspots, suggesting hotspots from persistent genera, rather than introduced genera. Hotspots were more similar to coldspots than background, suggesting coldspots may represent dying hotspots. Sample category predicted taxonomic similarity better than proximity, further indicating these heterogeneities are distinct from the background at the sub-centimetre scale. Hotspots and coldspots represent distinct spatial taxonomic distributions, rather than changes of the overall community. This suggests 0.3 ml volumes are cohesive long enough for particular operational taxonomic units (OTUs) to increase and create taxonomically distinct microscale communities within the Kolmogorov and Batchelor scales.

KEY WORDS: Microscale patchiness · Hotspots · Coldspots · Bacterioplankton · Species composition

Resale or republication not permitted without written consent of the publisher

INTRODUCTION

Bacteria are important for ecosystem function, playing a crucial role in the cycling of carbon, phosphorus and nitrogen (Azam 1998, Long & Azam 2001). It is at the microscale that these nutrient exchanges occur (Azam & Malfatti 2007, Stocker et al. 2008). Previously, microbial distributions were considered homogeneous or thought to follow patterns of random aggregation, leading to bulk phase sampling being considered representative of microbial microscale processes (Long & Azam 2001, Seymour et al. 2009, Dann et al. 2014). However within aquatic environments, it is now well accepted that microbial abundance and activity differ by orders of magnitude over µm to cm scales (Mitchell & Fuhrman 1989, Duarte & Vaqué 1992, Long & Azam 2001), with a previous study showing 45- and 2584-fold cm^{-1} variation in prokaryotic and viral abundance (Dann et al. 2014). In addition, recent work has shown that this patchiness also exists in freshwater systems, with river prokaryotic populations exhibiting up to an 80-fold change in abundance per 0.9 cm (Dann et al. 2016a).

*Corresponding author: lisa.dann@flinders.edu.au

© Inter-Research 2016 · www.int-res.com

Patchiness in microscale microbial distributions is typically characterised by abundance hotspots or coldspots. Hotspots are regions of elevated bacterial abundance resulting from microbial accumulation around high-nutrient areas via chemotaxis, particle aggregation or disintegration, small scale water mixing or grazing events in proximate areas. These high bacterial abundance regions have been suggested to result in increased viral production via lysis due to increased host density (Blackburn et al. 1998, Barbara & Mitchell 2003, Seymour et al. 2006). Coldspots are areas of lowered microbial abundance, believed to result from removal mechanisms such as lysis or grazing events in the case of lowered bacterial abundance, and attachment or grazing in regards to lowered viral abundance (Weinbauer & Höfle 1998, Wilhelm et al. 1998, Šimek et al. 2001). However, as previous studies of microscale prokaryotic distributions in freshwater systems have been limited to abundance estimates alone, whether hotspots and coldspots represent distinct spatial taxonomic distributions, and hence whether heterogeneous species richness and composition exists in freshwater, have remained unknown.

Within marine systems, Long & Azam (2001) analysed 16s rRNA gene diversity and richness using µl samples of seawater to test for small-scale patchiness in bacterial species. Their results indicated microscale variation in the bacterial community richness of the ocean down to the Kolmogorov and Batchelor scales, yet no similar investigation exists for freshwater. Therefore, the aim of this study was to determine whether microscale variation in species richness and composition occurs in freshwater systems, and confirm whether microscale patches represent distinct communities. We hypothesised that hotspots, coldspots and background represent distinct spatial taxonomic distributions, where hotspots are representative of distinct abundance increases of individual taxa. We tested this hypothesis by analysing the taxonomic composition of multiple hotspots, coldspots and background samples. From this, potential taxonomic patterns within these microenvironments were determined.

MATERIALS AND METHODS

Sample collection

Samples were collected from the Murray River at Murray Bridge, South Australia (35° 07′ 07″ S, 139° 16′ 56″ E) on 2 July 2014. At the time of sampling, the water temperature was 13.6°C, pH was 7.8, total dissolved solids was 445 mg l^{-1} and electrical conductivity was 445 µS cm^{-1}. Daily summary data showed a water depth of 0.66 m (Long Island Site ID: A4261162) (DEWNR 2014). All environmental parameters were measured using a HydroLab DataSonde probe.

A 2-dimensional sampling device (Dann et al. 2014) was employed enabling the collection of 8 vertical profiles with 0.9 cm separation and containing 12 sample points from 1.4 to 11.3 cm from the sediment–water interface of the river bed. This 96-well microplate collected approximately 300 µl per sample well.

For taxonomic analysis, 100 µl samples were collected from each microplate well, aliquoted into cryovials, immediately snap-frozen in liquid nitrogen and stored at −80°C until further analyses. For flow cytometric enumeration of prokaryotic and viral abundances, 200 µl samples were collected from each microplate well, immediately fixed with glutaraldehyde (0.5% final concentration) and stored at 4°C in the dark for 15 min. Samples were snap-frozen in liquid nitrogen and stored at −80°C until required for further analyses. Samples were processed within 1 wk of storage to avoid potential deterioration (Brussaard 2004).

Flow cytometry bacterial and viral abundance sample preparation, processing and analysis

Triplicate flow cytometry samples were prepared as described previously. Briefly, thawed samples were diluted 1:100 in Tris-EDTA buffer (0.2 µm filtered, pH 8.0, 10 mM Tris, 1 mM EDTA) and stained with SYBR Green I nucleic acid dye (1:20 000 final dilution; Molecular Probes). To optimise viral counts, samples were incubated at 80°C in the dark for 10 min (Brussaard 2004). Each sample was run in triplicate to check method precision. Reference beads of 1 µm diameter (Molecular Probes) were added to act as an internal size and concentration standard with a final concentration of approximately 10^5 beads ml^{-1} $sample^{-1}$. Bead fluorescence and concentration were used to calibrate sample volume and target size (Brussaard 2004).

A FACSCanto II cytometer equipped with blue laser (488 nm, 20 mW, air-cooled) and a sheath fluid of phosphate-buffered saline (PBS) solution was used for sample analysis. Samples were run for 2 min at a low flow rate to obtain less than 1000 events s^{-1}. Green fluorescence (SYBR I), right-angle light scatter

(SSC) and forward-angle light scatter (FSC) were acquired for each sample. Triplicate blank control samples containing filtered Tris-EDTA buffer (0.2 µl filtered) stained with SYBR Green I were prepared following the aforementioned sample preparation and run during each flow cytometry session to eliminate potential background noise created via flow cytometer artefacts or sample preparation (Brussaard 2004).

Flow cytometric histograms and cytograms were exported as FCS 3.0 files and analysed via FlowJo (Tree Star) to enumerate the prokaryotic and viral populations present (Smith et al. 2015, Dann et al. 2016a). Viral and prokaryotic populations were determined via their position in biparametric cytograms of SYBR Green fluorescence and side scatter (SSC) and the presence of discrete peaks in monoparametric histograms of SYBR Green fluorescence. SSC and SYBR Green fluorescence were used as indicators of cell size and nucleic acid content (Brussaard 2004).

Flow cytometry data analysis and representation

Rank abundance graphs were used to determine hotspot, coldspot and background values (Dann et al. 2014, 2016a). Background values were determined according to Wiebe (1970) where the median (rather than the mean) within the dataset was used as the background since the data were not normally distributed. Background values exhibited a linear trend and hence were indistinguishable from a random distribution, whilst the hotspots were identified as the sample points that exceeded this linear fit (see Fig. S1 in the Supplement at www.int-res.com/articles/suppl/a077p065_supp.pdf). Lastly, the coldspot values were identified as sample points that fit a linear trend but exhibited gentler slopes than were observed in the background values due to small differences between adjacent sample points (Fig. S1). From this, 3 of the highest abundance hotspots (H1, H2 and H3), lowest abundance coldspots (C1, C2 and C3) and median background samples (B1, B2 and B3) were selected for taxonomic analysis. For the spatial relationship of these hotspot, coldspot and background samples, see Fig. 1C. Subpopulation correlations were determined via Pearson's coefficient with the a of 0.05 reduced by sequential Bonferroni correction (Holm 1979). All possible subpopulation correlations were analysed to identify potential relationships between the prokaryotic and viral subpopulations. Two-dimensional contour plots were constructed using Surfer 10 (Golden Software). When constructing these plots, a minimum contour interval value ≥1000 events ml^{-1} was chosen as this was higher than the maximum flow cytometric error, i.e. the background noise within triplicate blank control samples. This value is conservative due to the maximum flow cytometric error being <24 events ml^{-1}.

Quantitative PCR

The use of appropriate PCR reagents and sample volumes were trialled. To ensure sufficient prokaryotic amplification, different DNA sample volumes (1, 2, 3, 5, 10 and 23 µl) were analysed via quantitative PCR (qPCR). Briefly, 16s region-specific forward 27F (5′-AGR GTT TGA TCM TGG CTC AG-3′) and reverse 519R (5′-GTN TTA CNG CGG CKG CTG-3′) primers were added to 1 µl DNA samples stained with Universal KAPA SYBR Fast qPCR Master Mix 2x (KAPA Biosystems) and run through 42 qPCR cycles on a Rotor-Gene. SYBR quantitation reports using Rotor-Gene Real-Time Analysis Software (v.6.0.27) showed amplification in the 1 µl DNA samples whilst the 2, 3, 5, 10 and 23 µl samples were inhibited, perhaps due to the high level of tannins in the water samples (Kontanis & Reed 2006). To ensure 1 µl samples were representative, ten 1 µl samples were taken for the highest hotspot, lowest coldspot and mean background, whilst five 1 µl samples were taken for the remaining 2 hotpots, coldspots and background samples; taxonomic analysis was performed on each sample.

Direct PCR amplification of bacterial communities

Direct PCR amplification was performed on 1 µl samples in 25 µl PCR reactions that consisted of KAPA Taq Ready Mix 2x (KAPA Biosystems), and forward (27F) and reverse (519R) primers specific to the 16s sequence region. Samples were run on a Veriti 96 well Thermal Cycler (Applied Biosystems) for 42 cycles consisting of 3 stages. Of the resulting PCR products, 5 µl was run on an electrophoresis agarose gel to ensure adequate DNA amplification and 20 µl was used for 16s rRNA sequencing. Negative controls were run with sterile filtered water in place of template. For sequencing, the variable 16s rRNA gene region PCR primers with forward primer barcodes were used in a 5 cycle PCR using HotStarTaq Plus Master Mix Kit (Qiagen) with the following conditions: 94°C for 3 min, followed by 28 cycles at 94°C

for 30 s, 53°C for 40 s, 72°C for 1 min and a final elongation step at 72°C for 5 min. PCR products were run on a 2% agarose gel to determine amplification success and relative band intensity. Barcoded samples were pooled together in equal proportions based on molecular weight and DNA concentrations and then purified via calibrated Ampure XP beads. Sequencing was performed at Molecular Research (Shallowater) on an Illumina MiSeq following the manufacturer's guidelines.

Taxonomic analysis

Sequenced bacterial DNA was quality-filtered and length-truncated with reads <250 bp or containing >0.5% expected errors for all bases discarded. Sequences lacking a recognisable barcode or forward PCR primer were also discarded. The USEARCH pipeline was employed for full length de-replication and abundance sorting using a minimum size of 2 to ensure singleton removal (Edgar 2010). Removal of singletons ensured that spurious operational taxonomic units (OTUs) resulting from PCR errors and/or sequencing artefacts were discarded (Edgar 2013, Liu et al. 2015). OTU clustering at 97% identity was performed via the 'cluster_otus' command using UPARSE in USEARCH v.8 (Edgar 2013). Reference-based chimeric filtering was carried out using the gold database via UCHIME (Edgar et al. 2011, Pylro et al. 2014). Reads were then globally mapped to the OTUs using 97% identity threshold, and taxonomic assignment was performed using RDP Classifier via the 'utax' command in USEARCH v.8 (Wang et al. 2007, Edgar 2013). OTU tables were constructed using python scripts, and the resulting OTU tabbed text file was used to determine average OTU abundances.

OTU tables were analysed in PRIMER (version 7) where square root overall transformed data was used for similarity percentage (SIMPER) analysis (Clarke & Gorley 2006). SIMPER was used to determine what is driving Bray-Curtis dissimilarity within and between sample values. Bray-Curtis resemblance was performed to construct dissimilarity matrices for PERMdisp, which was used to determine the level of dispersion between samples (Clarke 1993). Bray-Curtis resemblance of presence vs. absence was used to determine sample exclusivity of bacterial sequences. Metric multidimensional scaling (MDS) using bootstrap average analysis was performed to determine the level of spread between samples and produce smoothed 95% bootstrap regions for each sample type. Metric MDS ordination employed 500 bootstrap averages of the centroid of each sample to show where 95% of the centroid averages lay within multivariate space.

RESULTS

Prokaryotic and viral enumeration and 2-dimensional distributions

Flow cytometric analysis revealed 2 viral (V1 and V2) and 2 prokaryotic (low DNA [LDNA] and high DNA [HDNA]) subpopulations via dense regions in biparametric cytograms of SYBR Green fluorescence and side-scatter (see Fig. S2 in the Supplement at www.int-res.com/articles/suppl/a077p065_supp.pdf). Viral abundances ranged from 2.5×10^5 to 2.4×10^7 particles ml^{-1} (mean = 2.9×10^6, SD = 3.2×10^6, n = 95) for the V1 subpopulation, from 4.5×10^4 to 8.6×10^6 particles ml^{-1} (mean = 1.0×10^6, SD = 1.1×10^6, n = 95) for the V2 subpopulation and from 2.9×10^5 to 3.3×10^7 particles ml^{-1} (mean = 4.0×10^6, SD = 4.2×10^6, n = 95) for total viruses. Prokaryotic abundances ranged from 5.6×10^6 to 3.6×10^7 cells ml^{-1} (mean = 1.7×10^7, SD = 8.7×10^6, n = 95) for the LDNA subpopulation, from 3.4×10^6 to 1.4×10^7 cells ml^{-1} (mean = 7.4×10^6, SD = 2.8×10^6, n = 95) for the HDNA subpopulation and from 9.2×10^6 to 4.6×10^7 cells ml^{-1} (mean = 2.5×10^7, SD = 1.1×10^7, n = 95) for total prokayotes. One sample well was empty after water collection, providing a total of 95 samples from the 96-well microplate.

The 2-dimensional distributions of prokaryotes and viruses were characterised by hotspots and coldspots in abundance (Figs. 1 & S2). V1 had a maximum hotspot of 2.4×10^7 particles ml^{-1} and a minimum coldspot of 2.5×10^5 particles ml^{-1}, resulting in an overall 97.5-fold change in abundance over the sampling area. V2 had a maximum hotspot of 8.8×10^6 particles ml^{-1} and a minimum coldspot of 4.5×10^4 particles ml^{-1} resulting in an overall 195.4-fold change in abundance over the sampling area. LDNA had a maximum hotspot of 3.6×10^7 cells ml^{-1} and a minimum coldspot of 3.7×10^6 cells ml^{-1} resulting in a 9.7-fold change in abundance over the sampling area. HDNA had a maximum hotspot of 1.4×10^7 cells ml^{-1} and a minimum coldspot of 2.7×10^6 cells ml^{-1} resulting in a 5.2-fold change in abundance over the sampling area. From one sampling well to the next, the largest change in abundance for V1 was 84.2-fold, V2 was 115-fold, LDNA was 5.9-fold, HDNA was 3.7-fold, total viruses was 90.6-fold and total

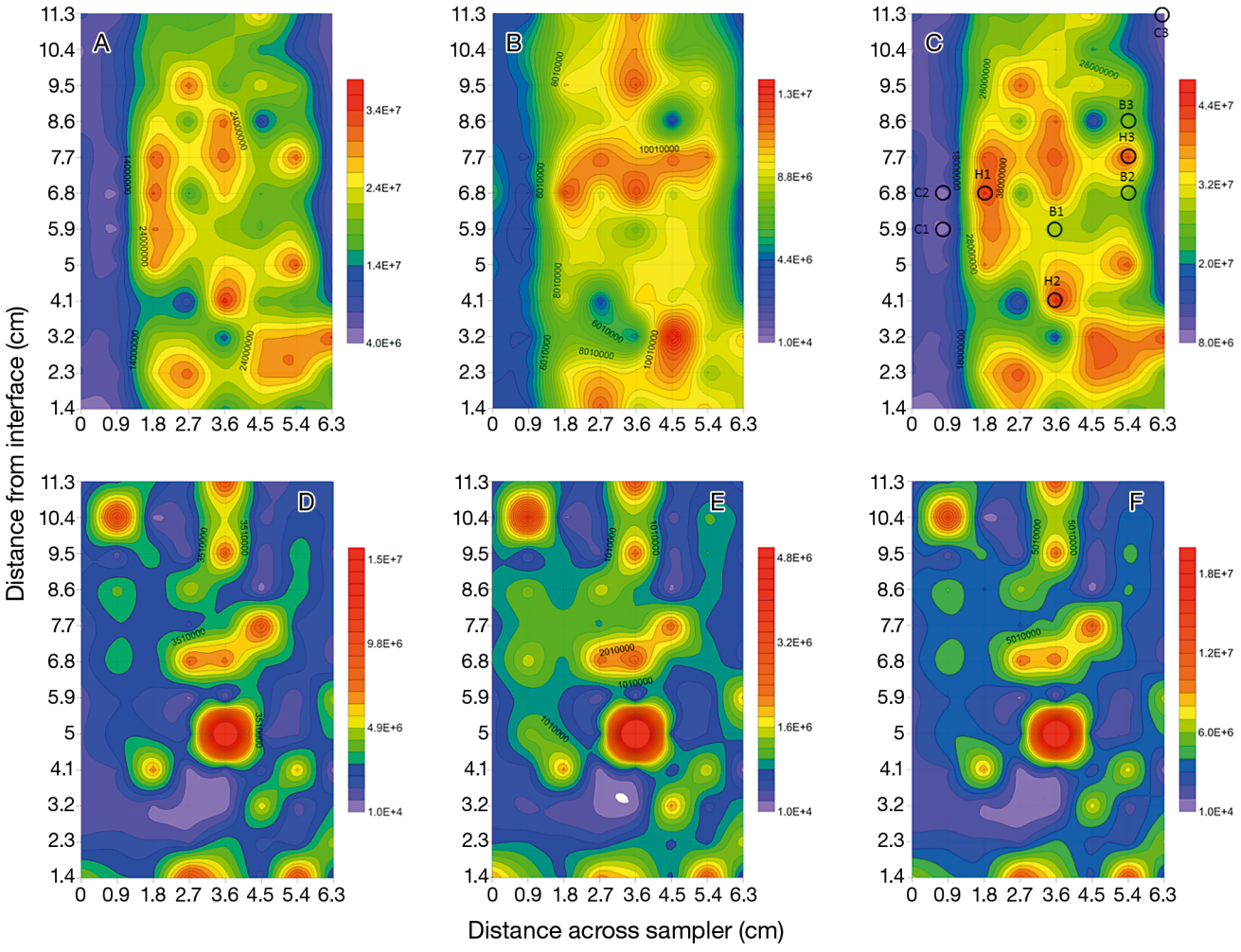

Fig. 1. Two-dimensional contour plots showing the presence of hotspots (H1–H3), coldspots (C1–C3) and background (B1–B3) in (A) low DNA (LDNA), (B) high DNA (HDNA), (C) total prokaryotes, (D) virus-1 (V1), (E) virus-2 (V2) and (F) total viruses. Faint gridlines indicate sampling interval; vertical profiles are separated by 0.9 cm. Colour intensity scale in cells or viruses ml^{-1}. Circles in (C) indicate sample location and corresponding label

prokaryotes was 4.5-fold per 0.9 cm. In addition, vertical gradients were present within the prokaryotic subpopulations with low abundance values in one of the bordering vertical profiles within the LDNA, HDNA and total prokaryotes, resulting in an up to 6-fold change in abundance over the 6.8 cm horizontal sampling distance (Fig. 1).

Correlations

Of the 56 total subpopulation vertical profile correlations, the single vertical profiles of V1 and V2 were positively correlated to one another in all 8 vertical profiles ($r^2 \geq 0.94$, n = 12, $p < 0.0001$), whereas 4 out of the 8 possible single vertical profiles of LDNA and HDNA were positively correlated ($r^2 \geq 0.72$, n = 12, $p \leq 0.009$). The remaining prokaryotic and viral single vertical profiles were not significantly correlated (Table S1 in the Supplement).

Taxonomic profiles

Hotspots

At the genus level, averaged hotspots contained an abundance of *Geothrix* (12.7%), *Nocardioides* (9.1%), *Flexibacter* (7.8%), *Chryseoglobus* (5.6%), *Thiobacillus* (4.9%), *Bacteroides* (4.8%), *Pseudomonas* (4.3%) and *Planctomyces* (4.1%) (Fig. 2A; Table S2 in the Supplement). SIMPER analysis of the hotspots at the genus level revealed a similarity of 55.4, with *Geothrix*, *Nocardioides* and *Chryseoglobus* being the

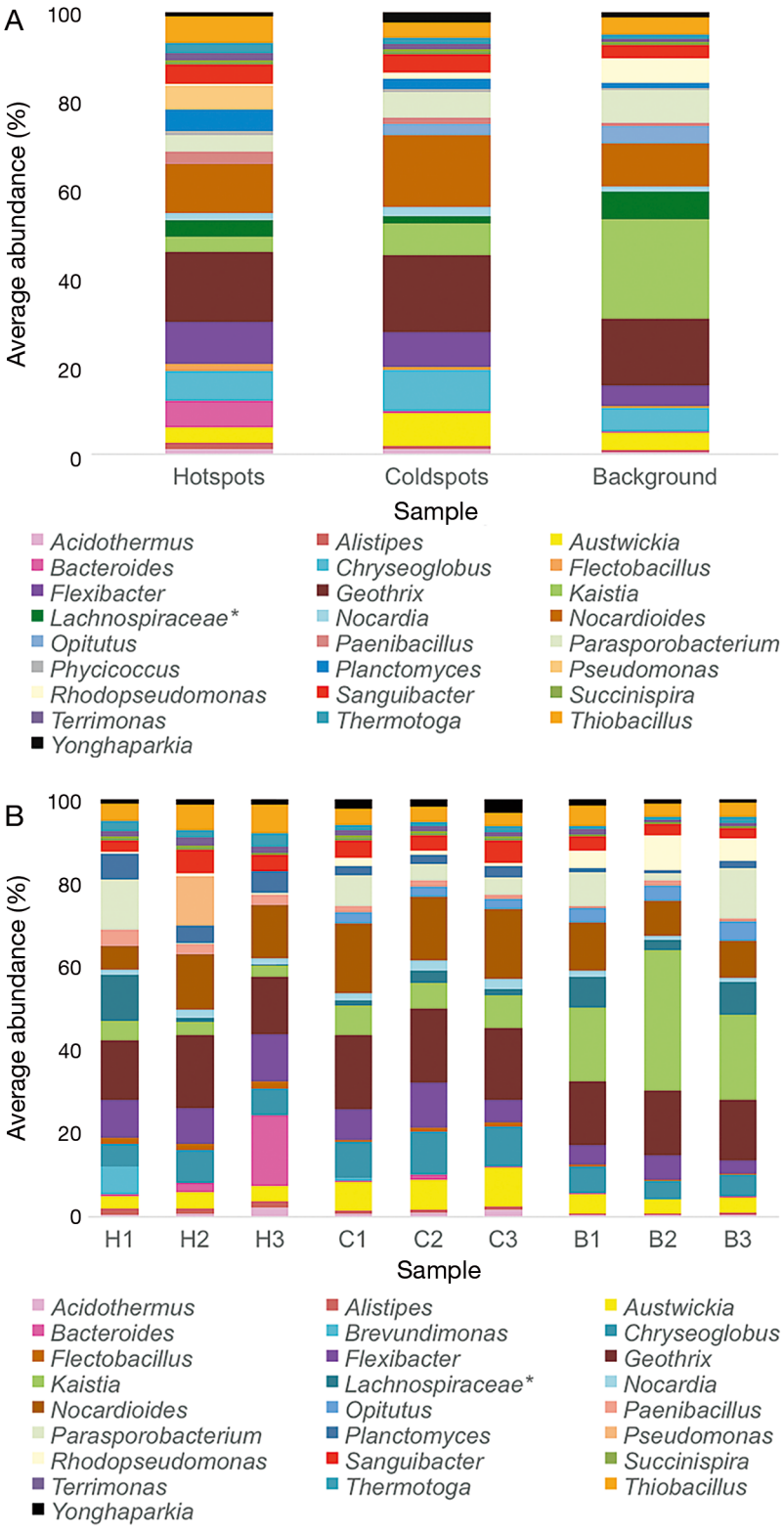

Fig. 2. Average abundance taxonomic profiles at the genus level of (A) averaged hotspot (n = 3), coldspot (n = 3) and background (n = 3) samples, and (B) individual hotspot (H1, H2 and H3), coldspot (C1, C2 and C3) and background (B1, B2 and B3) samples. For clarity, genera representing <2 and <6% total average abundance were omitted. *: incertae sedis

main contributors, contributing to >5% similarity. PERMdisp analysis showed an average dispersion of 30.3 (SE = 2.7).

Phylogenetic average abundance analysis of the averaged hotspots showed a high occurrence of *Proteobacteria* (28.9%), *Actinobacteria* (21.9%), *Bacteroidetes* (20.0%) and *Acidobacteria* (10.1%), with phyla dominance less obvious in the hotspots, as *Proteobacteria* had an average abundance of 7.0 and 8.9% above the second and third most abundant phyla, *Actinobacteria* and *Bacteroidetes* (Fig. S3A, Table S2 in the Supplement).

Genera profiles of individual hotspots showed a higher average abundance of *Pseudomonas* (9.4%) in H2, *Parasporobacterium* (10.2%) and *Lachnospiraceae* incertae sedis (9.4%) in H1 and *Bacteroides* (14.2%) in H3 (Fig. 2B; Table S3 in the Supplement). At the phyla level, there was a higher occurrence of *Proteobacteria* (33.0%) in H2, *Firmicutes* (20.2%) in H1 and *Bacteroidetes* (29.2%) in H3 (Fig. S3B). At the genus level, SIMPER analysis of the individual samples revealed similarities of 61.2 for H3, 53.3 for H2 and 57.5 for H1. Between sample positions there was lower dissimilarity between H1 and H3 than H3 and H2 and H1 and H2 (Table S4 in the Supplement). The main contributor to dissimilarity between the hotspot samples were *Bacteroides* and *Parasporobacterium*, which contributed to >3% dissimilarity. SIMPER analysis of presence vs. absence revealed an average similarity of 56.5. Between H1 and H3, H3 and H2 and H1 and H2, the number of exclusive genera were 35, 15 and 24, respectively (Tables S4 & S5).

Coldspots

At the genus level, averaged coldspots contained an abundance of *Geothrix* (15.7%), *Nocardioides* (14.7%),

Chryseoglobus (8.3%), *Flexibacter* (7.0%), *Austwickia* (6.7%), *Kaistia* (6.3%) and *Parasporobacterium* (5.1%) (Fig. 2A, Table S2). SIMPER analysis at the genus level revealed a similarity of 69.8, with the main contributors *Nocardioides* and *Geothrix* contributing to >5% similarity. PERMdisp analysis showed an average dispersion of 20.7 (SE = 1.1). Phylogenetic profiles of the averaged coldspots showed an abundance of *Actinobacteria* (37.0%), *Proteobacteria* (19.3%), *Acidobacteria* (13.8%) and *Bacteroidetes* (13.8%), with the most dominant phyla in the coldspots, *Actinobacteria*, representing 17.7% more than the second most abundant phyla (Fig. S3A, Table S2).

At the genus level, SIMPER analysis of the individual samples revealed similarities of 70.3, 71.6 and 66.0 for C2, C1 and C3, with a lower dissimilarity between C1 and C2 than C1 and C3 and C2 and C3 (Table S4). *Parasporobacterium* was the main contributor to dissimilarity between coldspot samples, accounting for ≥1.6% dissimilarity. SIMPER analysis of presence vs. absence revealed an average similarity of 75.2.

Background

At the genus level, averaged background samples had an abundance of *Kaistia* (19.9%), *Geothrix* (13.2%), *Nocardioides* (8.7%), *Parasporobacterium* (6.4%), *Lachnospiraceae* incertae sedis (5.4%), *Chryseoglobus* (4.9%) and *Flexibacter* (4.1%) (Fig. 2A, Table S2). SIMPER analysis at the genus level revealed a similarity of 74.3, with *Kaistia* and *Geothrix* (the main contributors to similarity) accounting for 6.2 and 5.3% similarity. PERMdisp analysis at the genus level revealed an average dispersion of 17.7 (SE = 0.4). Phylogenetic profiles of the averaged background values showed an abundance of *Proteobacteria* (37.2%), *Actinobacteria* (22.6%), *Firmicutes* (13.3%) and *Acidobacteria* (12.2%), with the most abundant phyla, *Proteobacteria*, represented 14.6% more than the next abundant phyla (Fig. S3A, Table S1).

At the genus level, SIMPER analysis of the individual samples revealed similarities of 76.2, 74.6 and 74.1 for B1, B2 and B3, with a lower dissimilarity between B1 and B3 than B2 and B3 and B2 and B1 (Table S4). *Lachnospiraceae* incertae sedis was the main contributor to dissimilarity between the background samples, accounting for ≥3.7% dissimilarity. SIMPER analysis of presence vs. absence revealed an average similarity of 77.3. In all instances — hotspots, coldspots and background — the most abundant *Proteobacteria* was *Alpha-* followed by *Betaproteobacteria* (Fig. S4 in the Supplement). No archaea were identified in the taxonomic profiles. Sequence quality filtering, chimera detection, read lengths and OTU classification results are provided in the Supplement.

Sample type comparisons

SIMPER analysis at the genus level revealed the highest level of dissimilarity (51.0) and genera exclusivity between the averaged hotspots and background, with *Kaistia*, *Thiobacter* and *Thiobacillus* contributing to >2.2% of this dissimilarity (Tables S4 & S6). The dissimilarity (47.2) and genera exclusivity between the averaged hotspots and coldspots was the second highest, with *Parasporobacterium* and *Opitutus* contributing to >1.7% of the dissimilarity (Tables S4 & S6). The averaged coldspots and background had the lowest level of dissimilarity (39.6) and genera exclusivity, with *Kaistia*, *Thiobacillus* and *Thiobacter* contributing to >2.5% of this dissimilarity (Tables S4 & S6).

Metric MDS analysis showed a difference between sample types with higher spread between hotspots rather than coldspots and background (Fig. 3).

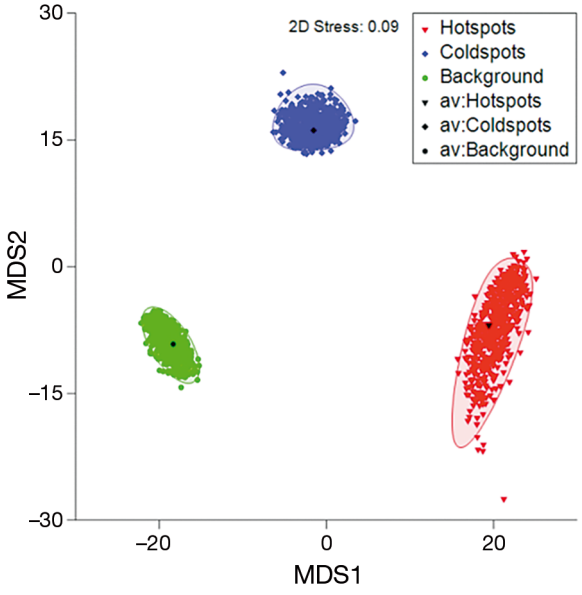

Fig. 3. Metric multidimensional scaling (MDS) analysis of sample type, hotspot (red triangles), coldspot (blue diamonds) or background (green circles). Metric MDS ordination employed 500 bootstrap averages of the centroid of each sample to show where 95% of the centroid averages lie within multivariate space

Proximate samples

Proximate samples were compared to determine whether a spatial component was present within the taxonomic profiles. At the genus level, SIMPER analysis of proximate coldspots and hotspots revealed an average dissimilarity of 29.2 between samples C2 and C1, 47.2 between samples C2 and H1 and 46.1 between samples C1 and H1. *Parasporobacterium* contributed to > 2.5% dissimilarity between the coldspot samples, while *Parasporobacterium*, *Lachnospiraceae* incertae sedis and *Nocardioides* contributed to >1.9% dissimilarity between coldspot and hotspot samples. SIMPER analysis of presence vs. absence data showed a higher dissimilarity and exclusivity between proximate hotspots and coldspots, rather than proximate coldspots, with 94 and 103 genera exclusive between C1 and H1 and C2 and H1, and only 17 genera exclusive between C1 and C2 (Tables S4 & S5).

At the genus level, SIMPER analysis of the proximate background and hotspot samples showed a higher dissimilarity between hotspots and background, rather than background samples (Table S4). *Lachnospiraceae* incertae sedis and *Kaistia* accounted for ≥ 3.6% dissimilarity between the background samples, while *Kaistia* and *Bacteroides* contributed to ≥ 3.4% dissimilarity between background and hotspot samples.

SIMPER analysis of presence vs. absence data also showed a higher dissimilarity and exclusivity between hotspots and background rather than background samples (Tables S4 & S6), with 81 and 115 genera exclusive between hotspot and background samples compared to 18 genera between the background samples (Tables S4 & S6).

DISCUSSION

Microscale viral and prokaryotic distributions — hotspots, coldspots and surface gradients

Hotspots and coldspots were present in prokaryotic and viral microscale distributions near to the sediment–water interface of the river bed (Fig. 1). These patchy distributions in prokaryotic and viral abundance appear ubiquitous, having previously been found in a number of studies (Seymour et al. 2007, Stocker et al. 2008, Dann et al. 2014). In addition to hotspots and coldspots, surface abundance gradients were present within the prokaryotic subpopulations (Fig. 1). Surface abundance gradients relate to organic matter sinking and its incorporation into the benthos allowing its degradation and transformation by bacteria, therefore resulting in high nutrient concentrations at the sediment–water interface and hence high microbial abundance (Seymour et al. 2007). Unlike previous observations, the gradients observed here were vertical to the sediment–water interface and characterised by decreased rather than increased abundance (Seymour et al. 2007, Dann et al. 2014). Here, the decrease was 6-fold over 6.8 cm, whereas previously the increases were 2- to 15-fold over 15 and 11.3 cm sampling distances (Seymour et al. 2007, Dann et al. 2014). The lower abundance in these observed gradients implies a gradient of a different mechanism, perhaps extensive lysis via phage, or non-selective grazing via protists, with the latter being favoured due to a lack of correlation between viral and prokaryotic abundances within this gradient (Weinbauer & Höfle 1998).

A maximum abundance variation of 115-fold above background over 0.9 cm was observed in V2, which is similar to the maxima of 107-fold above background over 0.9 cm observed recently in the same river environment (Dann et al. 2016a), suggesting there is viral spatial heterogeneity within this river system. A maximum 5.9-fold change per 0.9 cm in abundance observed in prokaryotic subpopulations is much lower than the previous reported maxima of 80.5-fold per 0.9 cm (Dann et al. 2016a), perhaps due to the surface gradients within the prokaryotic microscale distributions, as these would lead to a more gradual change in abundance over the sampling area. Vertical profiles of the viral subpopulations were positively correlated with one another in all instances, and half of the prokaryotic subpopulations profiles were positively correlated to each other. In contrast, the vertical profiles of prokaryotic and viral subpopulations showed no correlations. Prokaryotic subpopulation correlations could relate to stimuli responses, such as to particulate organic matter, nutrient gradients or hydrological conditions, leading to the formation of high abundance areas (Stocker et al. 2008), whilst positive correlations between V1 and V2 could indicate minimal ecological separation between the 2 subpopulations (Seymour et al. 2006). The lack of strong negative and positive correlations between viral and prokaryotic subpopulations may be due to temporal mismatch of the populations. However, it also suggests that grazers may be the dominant source of prokaryotic mortality, therefore releasing energy to higher trophic levels, and hence being the prevailing removal process for coldspot formation (Weinbauer & Höfle 1998, Tsai et al. 2013). In addition, observed viral subpopulations may have eukaryotic hosts, as has been found

in previous work by Parvathi et al. (2012), with the possible presence of algal viruses in the V1 region that do not respond to prokaryote population fluctuations. The lack of correlations might also indicate the ephemerality of heterogeneity where the diffusivity of viral progeny is low in comparison to potential bacterial motility rates, leading to high viral abundances in areas of past nutrient patches and prokaryotic hotspots (Seymour et al. 2006).

The viral and prokaryotic subpopulations were similar to those observed previously within the same environment from samples collected in 2012 (Dann et al. 2016a). However, mean viral concentrations were 20-fold lower for V1 and 19-fold lower for V2, despite both studies sampling during winter (Dann et al. 2016a). This difference in abundance may be due to the delivery of environmental water via flows and releases from locations upstream during 2013 and 2014, which resulted in higher flows to the South Australian portion of the Murray River sampled here (Burrell et al. 2014, DEWNR 2014). Despite this study and Dann et al. (2016a) sampling one spatial point, these results could potentially indicate that within this highly regulated river, viral abundance may be more dependent on annual river flow dynamics rather than seasonal variations typically observed in other freshwater studies (Walker & Thoms 1993, Maheshwari et al. 1995).

Hotspots and coldspots as distinct spatial taxonomic distributions

From early studies showing patchiness within plankton distributions (Birge 1897, Bainbridge 1957, Malone & McQueen 1983) to recent microscale work confirming patchiness in bacterial, viral and phytoplankton communities (Waters et al. 2003, Seymour et al. 2006, Dann et al. 2014) — whether this patchiness represented temporary abundance increases or distinct communities remained unknown. Here, we confirm that microscale microbial hotspots, coldspots and background regions represent distinct spatial taxonomic distributions (Fig. 3). Hotspots were characterised by distinct genera abundance increases, specifically *Parasporobacterium*, *Lachnospiraceae* incertae sedis, *Pseudomonas* and *Bacteroides* (Fig. 2B). Genera abundance increases differed between hotspot samples, leading to high dissimilarity with coldspots and background as well as other hotspot samples. Increases in specific genus abundance indicates exploitation of favourable environmental conditions, for instance fast moving motile bacteria taking advantage of ephemeral nutrient patches which other bacterial species may not have the speed to encounter in time (Seymour et al. 2006, Stocker et al. 2008). Success in competition could be coupled with the decline in other species, which would likely be due to selective grazing by protists or lysis by the phage of these non-successive species. Stocker et al. (2008) showed that some species of bacteria are capable of better exploiting ephemeral nutrient patches due to their motility rates, referred to as 'opportunitrophs'. This exploitation is possible for *Pseudomonas*, as well as some species of *Bacteroides,* as they are capable of motility (Shrout et al. 2006, McBride & Zhu 2013).

In addition, specific genus abundance increases may represent microbial associations with suspended particulate matter. For instance, within riverine systems, organic and inorganic suspended particles produced via auto- and allochthonous sources can harbour a range of microbial communities (Kernegger et al. 2009). Specifically, *Bacteroidetes* have been shown to colonise and dominate large particles due to their ability to grow whilst attached to particles (Fernández-Gómez et al. 2013). These particle-associated microbial communities contribute to a high proportion of activity and production (Iriberri et al. 1987, Griffith et al. 1990, Grossart & Simon 1993, 1998). Abundance increases of *Pseudomonas* may suggest microenvironments where this genus is able to out-compete other genera for a nutrient source, hence leading to its increased abundance. In addition, pseudomonads have the capacity to live anaerobically in biofilms (Hassett et al. 2002). Therefore, the abundance increases of *Pseudomonas* could indicate either biofilm aggregates or the exploitation of nutrient patches due to its motility.

Bacteroides are anaerobic and constitute the majority of mammalian gastrointestinal flora, playing an important role in the intestines. For this reason, *Bacteroides* have been used as faecal indicators in river systems, indicating the presence of mammalian faecal-associated particulate matter (Okabe et al. 2007). As the Murray River is impacted by human activity, the presence of mammalian faecal bacteria is expected.

The specific genera abundance increases in the hotspots, *Parasporobacterium* and *Lachnospiraceae* incertae sedis, are members of the *Firmicutes*, within the class *Clostridia*. *Parasporobacterium* are anaerobic bacteria typically found in freshwater sediments, and certain species, such as *P. paucivorans* are responsible for methanethiol and dimethyl sulphide formation via sulphide methylation (Lomans et al. 2001). Therefore, this increase in *Parasporobacterium* abundance could indicate sediment biofilm aggregates that had been resuspended into the water col-

umn. *Lachnospiraceae* incertae sedis are also anaerobic and are involved in biohydrogenation in rumens, indicating the presence of faecal particles from ruminant animals such as sheep and cattle, and therefore the potential impact of ruminant animals on the microbial river biota (Huws et al. 2011).

Hotspots and coldspots had higher similarity and lower exclusivity than hotspots and background, suggesting that coldspots are the result of dying hotspots, or that hotspots are the prolific growth of coldspots. For instance, coldspots may indicate the promotion of specific genera leading to the distinct genus abundance increases observed within the hotspots. Specific genus abundance increases and overall abundance increases may also occur where *Kaistia* has a lowered abundance. This genus was found in high abundances within background, but lowered abundance in coldspots and hotspots (Fig. 2). Therefore, hotspots and coldspots could indicate a reduction in the persistent and most abundant genera within background environments.

Here, we identified 52, 61 and 74 bacterial genera exclusive between hotspots and coldspots, hotspots and background and background and coldspots, respectively (Tables S4 & S6 in the Supplement at www.int-res.com/articles/suppl/a077p065_supp.pdf). Coldspots and background contained more exclusive genera than hotspots, indicating hotspots allow specific genera enrichment at the expense of genera diversity. As the genera exclusive to the hotspots were not the genera with increases in abundance causing the high dissimilarity between hotspots, coldspots and background, this indicates that hotspots are not exclusive representations of genera appearance, and further supports the notion that hotspots represent the enrichment of persistent genera. Therefore, it is the dominance or whether genera succeed within each microenvironment, rather than appearance or loss, which leads to the main differences between hotspots, coldspots and background.

By looking at adjacent samples, potential proximate relationships were determined. Lower similarity between proximate samples suggests sample proximity is not indicative of taxonomic and abundance similarity. Two coldspots proximate to a hotspot showed the highest similarity due to sample type, with higher similarity between the coldspots. The main drivers for dissimilarity between the coldspots and hotspot were *Parasporobacterium* and *Lachnospiraceae* incertae sedis, which had heightened abundance within hotspots, and *Nocardioides*, which was more abundant in coldspots. Higher dissimilarity between coldspots and hotspots were indicated by higher exclusivity in the coldspots, suggesting coldspots are high diversity yet low abundance microenvironments, whereas hotspots contain heightened abundance of bacteria that are common to coldspot samples.

Proximate background and hotspot samples also showed a higher similarity between samples of the same type rather than proximate samples of different type. A greater dissimilarity between sample types was due to *Kaistia* and *Bacteroides*, with the former more abundant within the background and the latter showing heightened abundance in hotspots. In addition to the heightened *Bacteroides* abundance was its low abundance in the background, which indicated the background does not provide an environment allowing *Bacteroides* enrichment. This could perhaps be due to competing bacterial genera, for instance *Kaistia*, as this genus had heightened abundance within the background but a lowered abundance in the hotspot. These proximate relationships indicate that sample types are a better indicator of taxonomic relatedness than sample proximity, hence showing that background, hotspots and coldspots contain distinct taxonomic profiles (Fig. 3).

Common background within microbial taxonomic profiles

Phylogenetic analysis of the hotspots, coldspots and background revealed a dominance of *Proteobacteria*, *Actinobacteria*, *Acidobacteria*, *Bacteroidetes* and *Firmicutes* (Fig. S3). Previous studies have shown *Proteobacteria*, *Actinobacteria* and *Cytophaga-Flavobacterium-Bacteroides* (CFB) are common freshwater microbial phylotypes (Zwart et al. 2002, Newton et al. 2006, Wu et al. 2007, Andersson et al. 2008, Ballesté & Blanch 2010). Dann et al. (2016) also found *Actinobacteria*, *Proteobacteria* and *Bacteroidetes* (filamentous bacteria associated with the human gut microbiota) to be abundant within the same river environment. *Acidobacteria* are less common in freshwater systems, yet Dann et al. (2016) identified an abundance of *Acidobacteria* during winter sampling of the Murray River (Zwart et al. 2002). At the genus level, hotspot, coldspot and background samples contained an increased presence of *Geothrix* and *Nocardioides*, as well as *Kaistia* within the background samples (Fig. 2). *Geothrix*, *Nocardioides* and *Kaistia* are typical freshwater sediment bacteria, suggesting their reincorporation/resuspension into the water column from the benthos (Coates et al. 1999, Topp et al. 2000, Jin et al. 2012). In addition, *Geothrix* species are associated with the breakdown of organic mate-

rial and Fe(III)-reduction and can assist in the oxidation of organic contaminants, and can therefore influence water quality, as has been observed in aquifers (Nevin & Lovley 2002). Species of the *Nocardioides* degrade numerous toxic organic pollutants, such as insecticides used in agricultural farming, thus implying a potential anthropogenic effect that persists at background levels (Topp et al. 2000).

Long & Azam (2001) hypothesised that using 1 µl samples in heterogeneous environments would enable better detection of rare phylotypes that would otherwise be missed if bulk phase sampling was used. Here, we show support for this hypothesis by obtaining >1244 OTUs by using 1 µl sample volumes, compared to a previous study within the same environment that obtained 613 OTUs using 5 l sample volumes (Dann et al. 2016). This indicates that taxonomic studies within heterogeneous environments, particularly those concerned with the rare biosphere, require small-scale sampling to achieve adequate sensitivity in taxonomic profiling. Furthermore, the size of the samples and the taxonomic differentiation within them indicates that microbial variation persists and is coherent down to and within the Kolmogorov and Batchelor scales (Duarte & Vaqué 1992, Seymour et al. 2004, 2005). The implication is that taxonomically and numerically stable microscale patches exist in at least some aquatic environments.

CONCLUSIONS

Here, we report that microscale microbial hotspot, coldspot and background regions are taxonomically distinct at all taxonomic levels. Abundance hotspots varied 115- and 5.9-fold above background over 0.9 cm for viruses and bacteria, respectively. These density differences were observed within a 0.9 cm distance and were characterised by distinct bacterial genera abundance increases. Moreover, predominant genera of bacteria differed among hotspots. Genera showing heightened abundance (specifically *Parasporobacterium, Lachnospiraceae* incertae sedis and *Bacteroides*) were indicative of animal and human inputs, indicating a potential anthropogenic effect on microbial patchiness. We have shown that volumes of less than 1 ml can have taxonomically distinct groupings and that these appear to remain coherent for extended periods. These findings suggest that community structure and heterogeneity exists within the Kolmogorov and Batchelor scales, which will therefore have a significant impact on local microbial biogeochemical cycling.

Acknowledgements. We thank Dr C. MacArdle and S. Bailey of the Flow Cytometry Unit of the Flinders Medical Centre, South Australia. This research was supported by a CSIRO Land and Water Top-Up PhD Scholarship (L.D.), a CSIRO consumables grant (L.D.), an APA to L.D. and Australian Research Council grants, www.arc.gov.au, LP-130100508 and DP-150103018 to J.G.M.

LITERATURE CITED

Andersson AF, Lindberg M, Jakobsson H, Bäckhed F, Nyrén P, Engstrand L (2008) Comparative analysis of human gut microbiota by barcoded pyrosequencing. PLOS ONE 3:e2836

Azam F (1998) Microbial control of oceanic carbon flux: the plot thickens. Science 280:694–696

Azam F, Malfatti F (2007) Microbial structuring of marine ecosystems. Nat Rev Microbiol 5:782–791

Bainbridge R (1957) The size, shape and density of marine phytoplankton concentrations. Biol Rev Camb Philos Soc 32:91–115

Ballesté E, Blanch AR (2010) Persistence of *Bacteroides* species populations in a river as measured by molecular and culture techniques. Appl Environ Microbiol 76: 7608–7616

Barbara GM, Mitchell JG (2003) Marine bacterial organisation around point-like sources of amino acids. FEMS Microbiol Ecol 43:99–109

Birge EA (1897) Plankton studies on Lake Mendota. II. The crustacea of the plankton, July, 1894 – Dec 1896. Trans Wis Acad Sci Arts Lett 11:274–448

Blackburn N, Fenchel T, Mitchell JG (1998) Microscale nutrient patches in planktonic habitats shown by chemotactic bacteria. Science 282:2254–2256

Brussaard CPD (2004) Optimisation of procedures for counting viruses by flow cytometry. Appl Environ Microbiol 70:1506–1513

Burrell M, Moss P, Petrovic J, Ali A (2014) General purpose water accounting report 2012-2013: NSW Murray catchment. NSW Department of Primary Industries, Sydney

Clarke KR (1993) Non-parametric multivariate analyses of changes in community structure. Aust J Ecol 18:117–143

Clarke KR, Gorley RN (2006) PRIMER v6: user manual/tutorial. PRIMER-E, Plymouth

Coates JD, Ellis DJ, Gaw CV, Lovley DR (1999) *Geothrix fermentans* gen. nov., sp. nov., a novel Fe(III)-reducing bacterium from a hydrocarbon-contaminated aquifer. Int J Syst Bacteriol 49:1615–1622

Dann LM, Mitchell JG, Speck PG, Newton K, Jeffries T, Paterson J (2014) Virio- and bacterioplankton microscale distributions at the sediment-water interface. PLOS ONE 9:e102805

Dann LM, Paterson JS, Newton K, Oliver R, Mitchell JG (2016a) Distributions of virus-like particles and prokaryotes within microenvironments. PLOS ONE 11:e0146984

Dann LM, Smith RS, Jeffries TC, McKerral JC, Fairweather PG, Oliver R, Mitchell JG (2016b) Persistence, loss and appearance of bacteria upstream and downstream of a river system. Mar Freshw Res

DEWNR (Department of Environment, Water and Natural Resources) (2014) River Murray Act annual report 2013-2014 and triennial review 2014. Department of Environment, Water and Natural Resources, Government of South Australia, Adelaide

Duarte CM, Vaqué D (1992) Scale dependence of bacterioplankton patchiness. Mar Ecol Prog Ser 84:95–100

Edgar RC (2010) Search and clustering orders of magnitude faster than BLAST. Bioinformatics 26:2460–2461

Edgar RC (2013) UPARSE: Highly accurate OTU sequences from microbial amplicon reads. Nat Methods 10:996–998

Edgar RC, Haas BJ, Clemente JC, Quince C, Knight R (2011) UCHIME improves sensitivity and speed of chimera detection. Bioinformatics 27:2194–2200

Fernández-Gómez B, Richter M, Schüler M, Pinhassi J, Acinas SG, González JM, Pedrós-Alio C (2013) Ecology of marine *Bacteroidetes*: a comparative genomics approach. ISME J 7:1026–1037

Griffith PC, Douglas DJ, Wainright SC (1990) Metabolic activity of size-fractionated microbial plankton in estuarine, nearshore, and continental shelf waters of Georgia. Mar Ecol Prog Ser 59:263–270

Grossart HP, Simon M (1993) Limnetic macroscopic organic aggregates (lake snow): occurrence, characteristics, and microbial dynamics in Lake Constance. Limnol Oceanogr 38:532–546

Grossart HP, Simon M (1998) Bacterial colonisation and microbial decomposition of limnetic organic aggregates (lake snow). Aquat Microb Ecol 15:127–140

Hassett DJ, Cuppoletti J, Trapnell B, Lymar SV and others (2002) Anaerobic metabolism and quorum sensing by *Pseudomonas aeruginosa* biofilms in chronically infected cystic fibrosis airways: rethinking antibiotic treatment strategies and drug targets. Adv Drug Deliv Rev 54: 1425–1443

Holm S (1979) A simple sequentially rejective multiple test procedure. Scand J Stat 6:65–70

Huws SA, Kim EJ, Lee MRF, Scott MB and others (2011) As yet uncultured bacteria phylogenetically classified as *Prevotella, Lachnospiraceae* incertae sedis, and unclassified *Bacteroidales*, *Clostridiales* and *Ruminococcaceae* may play a predominant role in ruminal biohydrogenation. Environ Microbiol 13:1500–1512

Iriberri J, Unanue M, Barcina I, Egia L (1987) Seasonal variation in population density and heterotrophic activity of attached and free living bacteria in coastal waters. Appl Environ Microbiol 53:2308–2314

Jin L, Kim KK, Lee HG, Ahn CY, Oh HM (2012) *Kaistia defluvii* sp. nov., isolated from river sediment. Int J Syst Evol Microbiol 62:2878–2882

Kernegger L, Zweimüller I, Peduzzi P (2009) Effects of suspended matter quality and virus abundance on microbial parameters: experimental evidence from a large European river. Aquat Microb Ecol 57:161–173

Kontanis EJ, Reed FA (2006) Evaluation of real-time PCR amplification efficiencies to detect PCR inhibitors. J Forensic Sci 51:795–804

Liu M, Hu P, Zhang G, Zeng Y and others (2015) Copy number variation analysis by ligation-dependent PCR based on magnetic nanoparticles and chemiluminescence. Theranostics 5:71–85

Lomans BP, Leijdekkers P, Wesselink JJ, Bakkes P, Pol A, van der Drift C, Op den Camp HJM (2001) Obligate sulphide-dependent degradation of methoxylated aromatic compounds and formation of methanethiol and dimethyl sulphide by a freshwater sediment isolate, *Parasporobacterium paucivorans* gen. nov., sp. nov. Appl Environ Microbiol 67:4017–4023

Long RA, Azam F (2001) Microscale patchiness of bacterioplankton assemblage richness in seawater. Aquat Microb Ecol 26:103–113

Maheshwari BL, Walker KF, McMahon TA (1995) Effects of regulation on the flow regime of the River Murray, Australia. Regul Rivers Res Manage 10:15–38

Malone BJ, McQueen DJ (1983) Horizontal patchiness in zooplankton populations in two Ontario kettle lakes. Hydrobiologia 99:101–124

McBride MJ, Zhu Y (2013) Gliding motility and por secretion system genes are widespread among members of the phylum *Bacteroidetes*. J Bacteriol 195:270–278

Mitchell JG, Fuhrman JA (1989) Centimetre scale vertical heterogeneity in bacteria and chlorophyll *a*. Mar Ecol Prog Ser 54:141–148

Nevin KP, Lovley DR (2002) Mechanisms for accessing insoluble Fe(III) oxide during dissimilatory Fe(III) reduction by *Geothrix fermentans.* Appl Environ Microbiol 68: 2294–2299

Newton RJ, Kent AD, Triplett EW, McMahon KD (2006) Microbial community dynamics in a humic lake: differential persistence of common freshwater phylotypes. Environ Microbiol 8:956–970

Okabe S, Okayama N, Savichtcheva O, Ito T (2007) Quantification of host-specific *Bacteroides-Prevotella* 16s rRNA genetic markers for assessment of fecal pollution in freshwater. Appl Microbiol Biotechnol 74:890–901

Parvathi A, Zhong X, Jacquet S (2012) Dynamics of various viral groups infecting autotrophic plankton in Lake Geneva. Adv Oceanogr Limnol 3:171–191

Pylro VS, Roesch LFW, Morais DK, Clark IM, Hirsch PR, Tótola MR (2014) Data analysis for 16s microbial profiling from different benchtop sequencing platforms. J Microbiol Methods 107:30–37

Seymour JR, Mitchell JG, Seuront L (2004) Microscale heterogeneity in the activity of coastal bacterioplankton communities. Aquat Microb Ecol 35:1–16

Seymour JR, Seuront L, Mitchell JG (2005) Microscale and small-scale temporal dynamics of a coastal planktonic microbial community. Mar Ecol Prog Ser 300:21–37

Seymour JR, Seuront L, Doubell M, Waters RL, Mitchell JG (2006) Microscale patchiness of virioplankton. J Mar Biol Assoc UK 86:551–561

Seymour JR, Seuront L, Mitchell JG (2007) Microscale gradients of planktonic microbial communities above the sediment surface in a mangrove estuary. Estuar Coast Shelf Sci 73:651–666

Seymour JR, Marcos, Stocker R (2009) Resource patch formation and exploitation throughout the marine microbial food web. Am Nat 173:E15–E29

Shrout JD, Chopp DL, Just CL, Hentzer M, Givskov M, Parsek MR (2006) The impact of quorum sensing and swarming motility on *Pseudomonas aeruginosa* biofilm formation is nutritionally conditional. Mol Microbiol 62: 1264–1277

Šimek K, Pernthaler J, Weinbauer MG, Hornák K and others (2001) Changes in bacterial community composition and dynamics and viral mortality rates associated with enhanced flagellate grazing in a mesoeutrophic reservoir. Appl Environ Microbiol 67:2723–2733

Smith RJ, Paterson JS, Sibley CA, Hutson JL, Mitchell JG (2015) Putative effect of aquifer recharge on the abundance and taxonomic composition of endemic microbial communities. PLoS ONE 10:e0129004

Stocker R, Seymour JR, Samadani A, Hunt DE, Polz MF (2008) Rapid chemotactic response enables marine bac-

teria to exploit ephemeral microscale nutrient patches. Proc Natl Acad Sci USA 105:4209–4214

Topp E, Mulbry WM, Zhu H, Nour SM, Cuppels D (2000) Characterization of *S*-triazine herbicide metabolism by a *Nocardioides* sp. isolated from agricultural soils. Appl Environ Microbiol 66:3134–3141

Tsai AY, Gong GC, Sanders RW, Huang JK (2013) Contribution of viral lysis and nanoflagellate grazing to bacterial mortality in the inner and outer regions of the Chingjiang River plume during summer. J Plankton Res 35:1283–1293

Walker KF, Thoms MC (1993) Environmental effects of flow regulation on the lower River Murray, Australia. Regul Rivers Res Manage 8:103–119

Wang Q, Garrity GM, Tiedje JM, Cole JR (2007) Naïve Bayesian classifier for rapid assignment of rRNA sequences into the new bacterial taxonomy. Appl Environ Microbiol 73:5261–5267

Waters RL, Mitchell JG, Seymour J (2003) Geostatistical characterisation of centimetre-scale spatial structure of *in vivo* fluorescence. Mar Ecol Prog Ser 251:49–58

Weinbauer MG, Höfle MG (1998) Significance of viral lysis and flagellate grazing as factors controlling bacterioplankton production in a eutrophic lake. Appl Environ Microbiol 64:431–438

Wiebe PH (1970) Small-scale spatial distribution in oceanic zooplankton. Limnol Oceanogr 15:205–217

Wilhelm SW, Weinbauer MG, Suttle CA, Jeffrey WH (1998) The role of sunlight in the removal and repair of viruses in the sea. Limnol Oceanogr 43:586–592

Wu X, Xi W, Ye W, Yang H (2007) Bacterial community composition of a shallow hypertrophic freshwater lake in China, revealed by 16S rRNA gene sequences. FEMS Microbiol Ecol 61:85–96

Zwart G, Crump BC, Kamst-van Agterveld MP, Hagen F, Han SK (2002) Typical freshwater bacteria: an analysis of available 16S rRNA gene sequences from plankton of lakes and rivers. Aquat Microb Ecol 28:141–155

Editorial responsibility: Rutger de Wit, Montpellier, France

Submitted: November 11, 2015; Accepted: May 30, 2016
Proofs received from author(s): July 19, 2016